Chapter 1

Preliminary Wind Tunnel and CFD Investigation

1.1 Introduction

The review of sail ‡ow research that was presented in Chapter ?? highlighted the lack of available data for sail sections and the limited understanding of the ‡ow features. Moreover there have been no wind tunnel tests conducted for downwind sail shapes (camber > 20%). This chapter describes preliminary wind tunnel tests and CFD results for a two-dimensional downwind sail section. The goal of the study was to obtain insight into the behaviour of two-dimensional sail ‡ows and to gain an initial guage of the performance of di¤erent turbulence models. This preliminary investigation was used to form the direction and goals of the subsequent research.

1.1.1 Wind tunnel setup

Wind tunnel experiments were carried out at the De Bray wind tunnel in the University of Auckland's Yacht Research Unit. This wind tunnel is a low-speed, closed loop facility with a test section of dimensions $768mm \pounds 615mm$, a maximum speed of $60m:s^{i1}$ and a maximum turbulence intensity of 1%. Figure 1.1 illustrates the model which is positioned on aerodynamic struts above the force balance which itself is mounted horizontally below the test section.

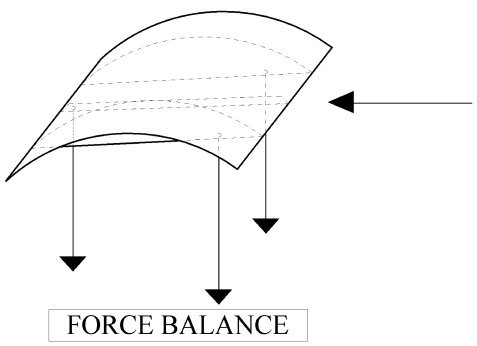

Figure 1.1: The wind tunnel model.

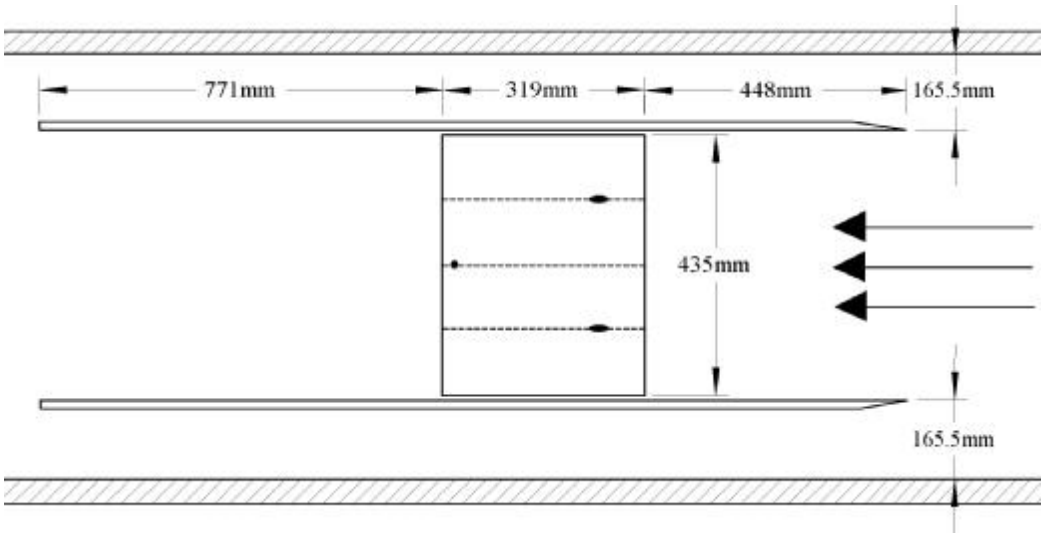

Figure 1.2: The wind tunnel model setup (from above, not to scale).

From analysis of IACC sail shapes it was evident that a circular arc represents a good approximation of a range of sail sections whilst providing a shape that is easy to manufacture. Therefore for this initial study a circular arc section was used with 24.7% camber, the model has a radius of 200mm and a chord length of 319*mm*. 1mm steel plate was rolled to the desired shape with a radial tolerance of less than 3mm which is equivalent to a camber variation of 0.6%. Steel strengthening sections were soldered to the underside of the model in order to minimize de‡ection under load and to provide an attachment point for the struts. Pitch was controlled using the rear strut and a rangle of di¤erent angles were investigated from $5^{\pm}$ through to $30^{\pm}$ at $2.5^{\pm}$ intervals.

The arrangement of the wind tunnel model within the tunnel is illustrated in Figure 1.2. At each end of the model end plates were positioned that span the height of the tunnel. These end plates were positioned 165.5*mm* inside the side walls of the tunnel to allow the boundary layer on the tunnel walls to pass without in‡uencing the model. The leading edges of the end plates were …xed at 448*mm* in front of the model and extend 711*mm* past the trailing edge. The model itself is 435*mm* (1:37*c*) wide and small gaps (< 2*mm*) exist between the tips of the model and the end plates. Tape and petroleum jelly were used to limit tip leakage through these gaps. Particular care was taken to ensure that friction between the model and the side walls did not in‡uence force measurements. This was veri…ed by measuring the forces when …xed weights were applied to the model.

The model was tested at an inlet speed of $25 m{:}s^{-1}$ which corresponds to a Reynolds number of $5.25 \pounds 10^5$. This Reynolds number is signi…cantly lower than the typical Reynolds number range of 2 ¡ 4 million for IACC sail ‡ows. However at these Reynolds numbers it is believed that the ‡ow should be reasonably independent of Reynolds number and validation of CFD models at the Reynolds number used in the wind tunnel should also apply to full scale sail ‡ows. The main reason that Reynolds number insensitvity can be expected is the presence of the leading edge separation bubble. As the shear layer separates at the leading edge transition occurs rapidly and conequently the boundary layer reattachment process is always turbulent and independent of Reynolds number. In the experimental study of ‡at plate leading edge bubbles of Crompton and Barrett the shear layer was observed to develop turbulent traits

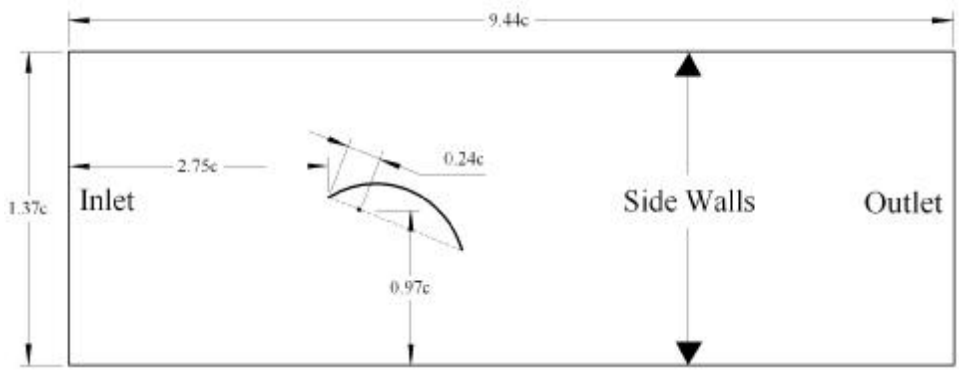

Figure 1.3: Details of the domain for the preliminary study.

shortly after detachment at the leading edge [1]. For that study Reynolds number independent results were obtained above a Reynolds number of $2.2 \pounds 10^5$.

1.1.2 The CFD Model

A schematic of the domain is illustrated in Figure 1.3. Due to the size of the model in relation to the wind tunnel dimensions it was felt that it was necessary to include the walls in the CFD model. Simulations were carried out using both non-slip and free-slip boundary conditions on the side walls and there was found to be no signi…cant loss in accuracy when free-slip conditions were used. Consequently free-slip boundary conditions were used for all simulations presented in this chapter. At the inlet the normal velocity was set to $5m:s^{\,i\,1}$ in order to mimic the Reynolds number of $5.25 \pounds 10^5$ that was used in the experiments. The tubulence intensity and length scale were set at 1% and $0.001m$ respectively. At the outlet a zero pressure gradient boundary condition was imposed.

Unfortunately since the model rotates in relation to the tunnel walls a new grid was required for each new angle of attack. The stuctured grids used in this study were generated using ICEM-HEXA. To ensure that the grids themselves were not a source of error a grid re…nement study was conducted (Section 1.2.1).Three levels of re…nement were used with the grids referred to as coarse, medium and …ne with 8496, 28912 and 120482 cells respectively and the medium grid is illustrated in Figure 1.4. At each re…nement level the number of nodes along every block boundary was doubled. In order to achieve a y^+ of approximately 1:0 the near wall spacing was set at $1{:}276 \pounds 10^{\,i\,5}c$. Particular care was taken to provide high quality cells around the leading and trailing edges and at the very ends of the sail the cells have an aspect ratio of 1 : 2:5. Away from the leading and trailing edges high aspect ratio cells are used in order to resolve the large ‡ow gradients normal to the wall.

1.2 Results

1.2.1 Convergence studies

Figure 1.5 shows the time-averaged force coe¢cients for the three grids at an angle of attack of 15 degrees which was felt to be a good representation of downwind sail ‡ows. The force coe¢cients are plotted against $1{=}N[m]$ which is a measure of the grid spacing where N^2 is the total number of cells in

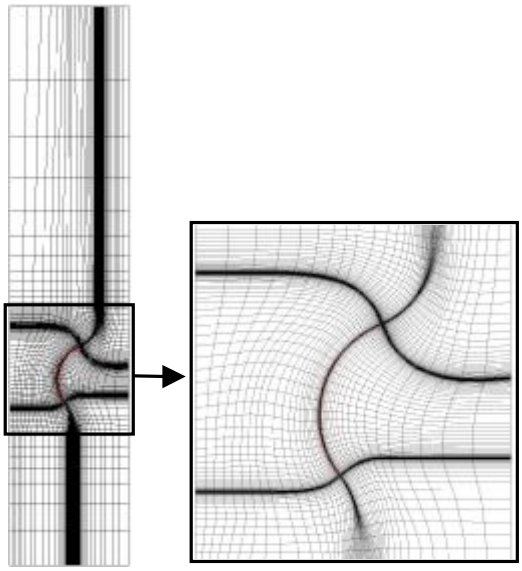

Figure 1.4: The computational grid for the preliminary study.

the grid. The medium grid produced a lift coe¢cient that was 1.6% smaller than the …ne grid result. Unfortunately halving the grid spacing again would result in a grid that would be impractical with regards to memory requirements and solution time. However for practical purposes the medium grid is acceptable and within 3% of the extrapolated value for lift.

A convergence study was also carried out on the time step. Solutions were compared using time steps of 0.025s, 0.0125s and 0.00625s. The lift coe¢cient calculated using the medium timestep was just 0.65% higher than the lift coe¢cient calculated using the short time step. For all simulations the 0.0125s was used for the timestep, this corresponds to approximately 32 iterations per period of vortex shedding. In all cases the simulations were run untill the solutions had settled into regular veroidic vortex shedding, i.e., the forces had constant means and amplitudes and the period of vortex shedding was was regular.

1.2.2 Wind tunnel - CFD comparison

CFD and wind tunnel time-averaged force coe¢cients are presented in Figure 1.6. In the experimental data a peak in the lift coe¢cient exists at 10 degrees which is associated with the so-called ideal angle of incidence where there is no leading edge bubble disrupting the ‡ow. There is a small drop o¤ in lift above 10 degrees associated with the formation of the leading edge bubble. Below 10 degrees the ‡ow stagnates on the leeward side and a separation bubble develops on the windward side of the sail, for ‡exible sails in this situation the lu¤ would collapse. Above 15 degrees the lift starts to increase again. At 30 degrees the model is fully stalled (totally separated ‡ow) and above this angle the lift coe¢cient is expected to drop o¤ once more.

The same trends are evident in the CFD results. The ideal angle of incidence is slightly lower (around 8 degrees) in the CFD, and at 30 degrees the lift curve for the SST model is starting to level o¤. At this angle the leading edge bubble detaches and reattaches in a semi-chaotic manner. At lower angles vortex shedding is regular and a vortex street exist in the wake (see Figure 1.7).

Downwind sails are trimmed to the lowest possible angle achievable without the lu¤ collapsing due

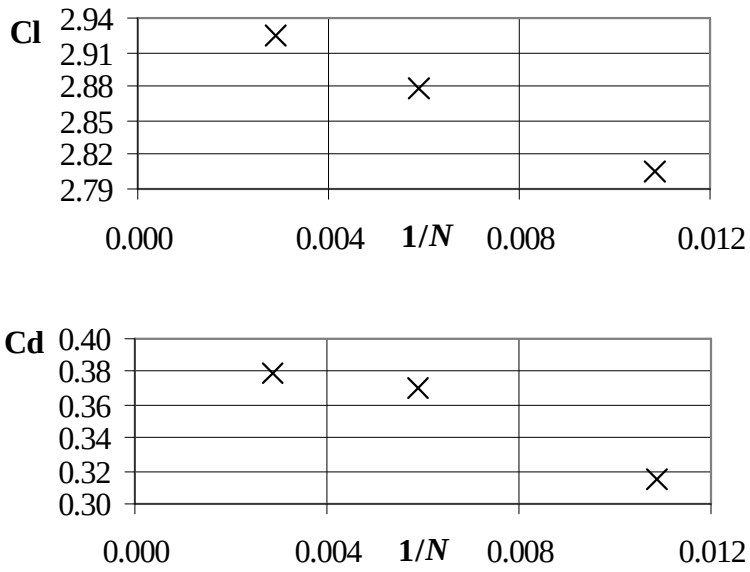

Figure 1.5: Grid convergence of the time-averaged lift and drag coe¢cients.

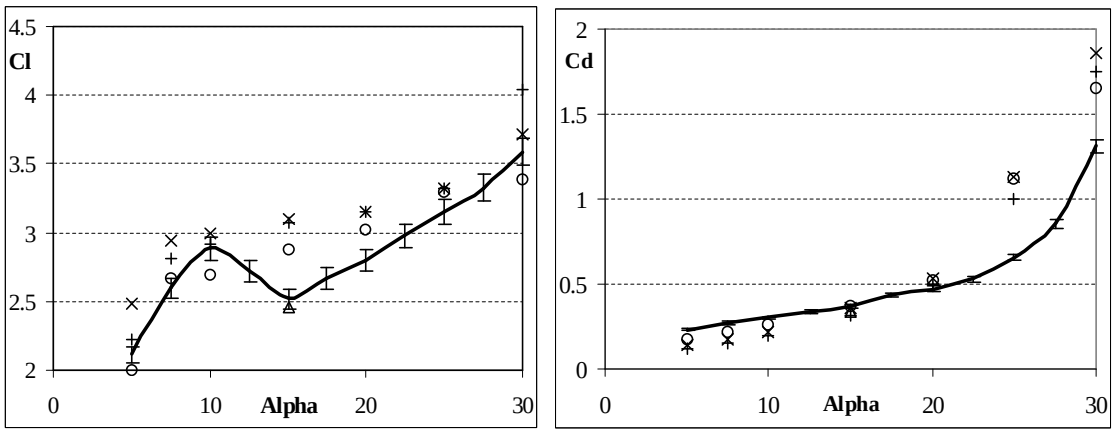

Figure 1.6: Force coe¢cients versus angle of attack (® = 15). —— Data, ± SST, + *k* ¡ *!*, £ *k* ¡ *²; ¢* 3D solution (SST).

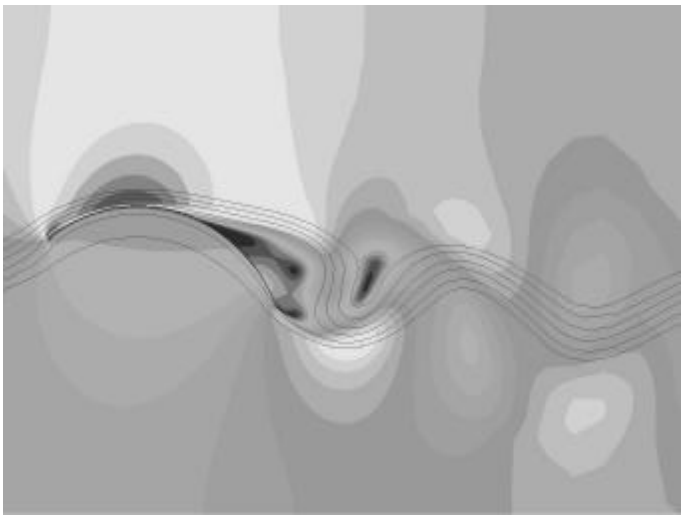

Figure 1.7: Velocity contours and streamlines (® = 15±).

to stagnation on the leeward side of the leading edge. Due to constantly ‡uctuating wind directions it is di¢cult to trim sails to ideal incidence and instead the sails are generally set at 5 – 10 degrees above the ideal angle of attack so that a stable lu¤ is maintained. If we assume an apparent wind of 90± so that we are looking to maximise lift while paying little attention to drag then Figure 1.6 would indicate that the sails should be trimmed to much higher angles of attack. However for the three-dimensional case there is considerable downwash due to tip vortices, consequently the ideal angle of attack is much higher and is closer to the angle of attack where real sails are fully separated (stalled). For real sails this means that maximum lift occurs at the ideal angle of incidence.

The general structure of the two-dimensional ‡ows - both in the wind tunnel and from CFD - compares well with streamlines visualised on three-dimensional model sails near mid-span. Figure 1.8 illustates a streamlines computed using CFD overlayed on a photo of smoke-lines from a three-dimensional wind tunnel test. Observations from smoke visualisation indicate that three-dimensional downwind sails generally separate at approximately 40-50% along the chord and two-dimensional CFD results (without mainsail) indicate that angles of attack of between 20 and 25 degrees are required in order to obtain this degree of separation.

In general the lift forces are overpredicted by CFD which is a commonly reported shortcoming of turbulence modelling. Overprediction of lift is due to large values of the eddy viscosity causing the boundary layer to remain attached in adverse pressure gradients that would normally cause separation. This e¤ect has been documented for many similar ‡ows such as the NACA 4412 airfoil at maximum lift [2]. However in such high-lift validation studies comparisons between CFD and experiment have shown much better agreement than the current comparison.

In our case the primary source of the error is attributed to three-dimensionality in the wind tunnel tests. Surface oil-‡ow visualisation was used and spanwise variation of the separation point was clearly apparent and surface tufts illustrated signi…cant cross-‡ow in the separated region near the trailing edge. Upstream of separation the ‡ow was nominally two-dimensional, although surface oil streams did bend slightly immediately upstream of the separation line. The three-dimensional structures present in the wake originate at the tunnel walls where the boundary layer on the wind tunnel wall interacts with the

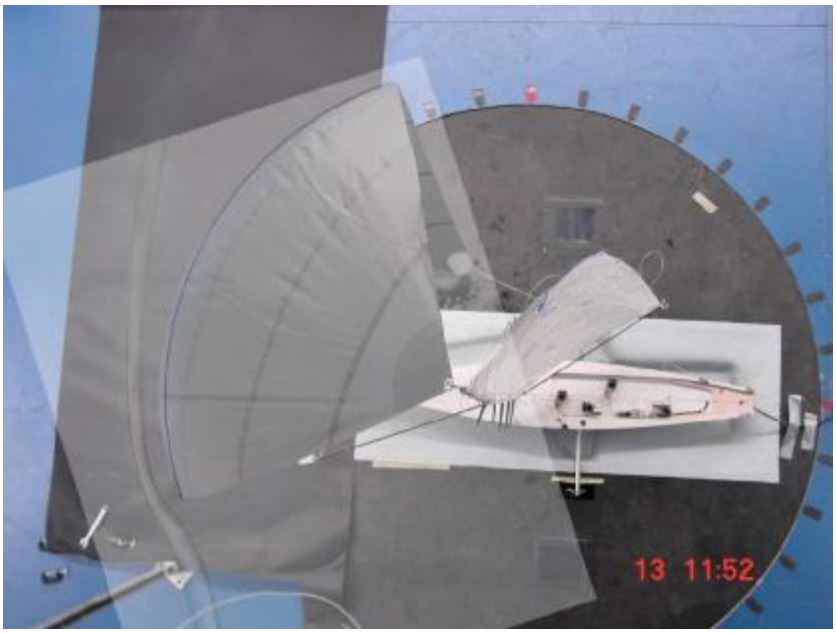

Figure 1.8: Wind tunnel ‡ow visualisation overlayed with streamlines computed using CFD.

boundary layer on the sail creating a horseshoe vortex around the leading edge of the sail. Consequently there is a greater degree of ‡ow separation near the tunnel walls. This e¤ect in‡uences the ‡ow right across the span of the sail.

A basic sketch of the ‡ow structure is illustrated in Figure 1.9. On the near side of the foil the ‡ow visualisation results are illustrated with the arrows representing the directions of surface tufts. Oil streaklines are also shown, upstream of the separation line. On the far side of the foil a schematic of the wake structure is illustrated. At approximately quarter and three-quarter span longitudinal vortices exist in the wake. This vorticity develops from the second (lower) separation bubble of the vortex pair.

This wake structure was con…rmed using a three-dimensional CFD model and the streamlines are illustrated in Figure 1.10. The grid that was used was based upon the coarse grid from the two-dimensional study, with 60 grid points in the spanwise direction and a symmetry plane was used at the midspan of the model. The surface plots of pressure coe¢cient and skin friction in Figure ?? illustrate spanwise variations and the skin friction contours closely follow the separation line patterns observed in the surface oil-‡ow visualisation.

The presence of the longitudinal counter rotating vortex pair causes downwash near mid span and upwash near the tunnel walls. Through examination of the streamlines upstream of the foil it is clear that the net e¤ect of the three-dimensional wake is to reduce the e¤ective angle of attack to the leading edge across the majority of the span. The leading edge bubble in the three-dimensional simulation is nominally two-dimensional and of almost constant length across 90% of the foil's span (the bubble breaks down near the side walls). At this angle of attack ($15^{\pm}$) the leading edge bubble reattaches at $0.033c$, for the equivalent two-dimensional simulation reattachment occurred at $0.077c$. The smaller leading edge separation bubble in the three-dimensional simulation is due to the lower e¤ective angle of attack imposed by the three-dimensionality of the wake.

From Figure 1.6 it is evident that the wind tunnel predicts the ideal angle of attack to be approximately

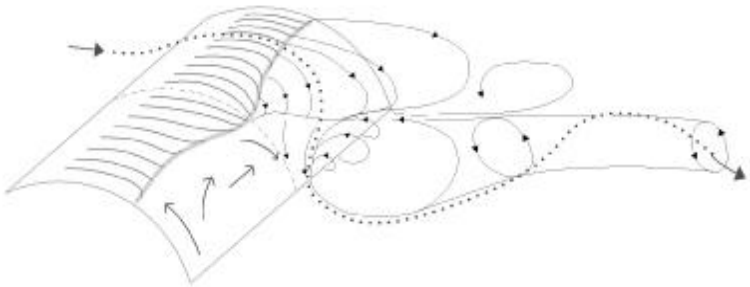

Figure 1.9: The wake structure.

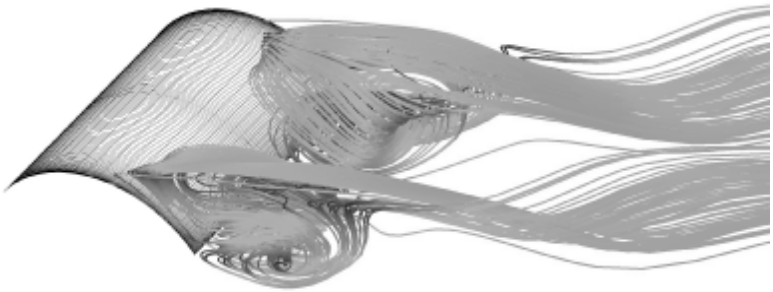

Figure 1.10: The wake structure computed by the 3D model, ® =15± (image re‡ected through symetry plane).

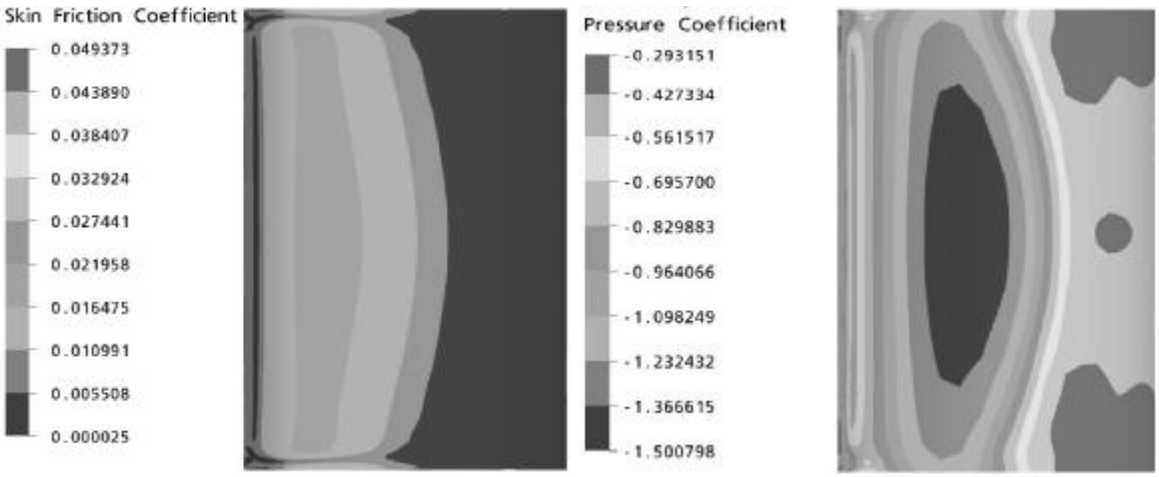

Figure 1.11: Suction side shear stress and pressure coe¢cient surface plots computed using the 3D model.

2 degrees higher than the CFD results indicate. This higher ideal angle of attack is due to downwash induced by the three-dimensional wake. Despite using tape to seal of the tips between the model the side walls, there is still likely to be a small amount of tip leakage. Flow visualisation was performed without tape sealing the tips and considerably more three-dimensionality was observed. Force measurements were also taken with the tape removed and the discrepancies with the CFD results were greater. Notably the ideal angle of attack was approximately 2.5 degrees higher than the previous wind tunnel experiments.

Unfortunately the errors caused by the three-dimensionality of the wind tunnel results are too large to allow reliable evaluation of the relative performances of the turbulence models. The forces from the three-dimensional CFD results (at $15^{\pm}$) were in better agreement with the wind tunnel experiments than the two-dimensional simulations. The lift was just 2.5% lower than the experimental results and the drag was 9.3% lower. However the grid was relatively coarse and no re…nement studies were performed. The grid re…nement study in Figure 1.5 indicates that the forces can be expected to rise with grid re…nement suggesting that a grid independent solution is likely to be even closer to the force values measured in the experiments. The three-dimensional simulations were performed primarily for visualisation and to aid understanding of this complex three-dimensional ‡ow. To draw stronger conclusions would require a more in-depth study of the three-dimensional ‡ow.

An attempt was made to record the Strohal number in the wind tunnel using a hot-wire anemometer positioned in the wake. However fourier analysis showed only low frequency modes which were attibuted to ‡uctuations of three-dimensional wake structures rather than unsteady vortex shedding. In order to determine the Strohal number - or even prove that unsteady vortex shedding is present for this ‡ow case - it is necessary to haev nominally two-dimensional ‡ow.

1.3 Conclusions

The main goal of the preliminary study was to was to obtain insight into the behaviour of two-dimensional sail ‡ows and to gain an initial guage of the performance of di¤erent turbulence models. Direct comparison between CFD and the wind tunnel tests was comprimised by the presence of signi…cant cross‡ow in the separated region of the wind tunnel model. Visualisation techniques were used to show that three-dimensional structures in the wake were dramatically altering the ‡ow and inducing downwash across the span of the model. Consequently the drag in the wind tunnel tests was increased and the lift decreased. A three-dimensional CFD simulation was performed in order to help visualise the wake structure and the computational model agreed well with the ‡ow visualisation performed in the wind tunnel. CFD proved to be a useful tool in gaining understanding of a particularily complicated ‡ow problem.

Due to an inability to produce nominally two-dimensional ‡ow the preliminary wind tunnel tests proved to be a poor test case for the validation of turbulence models. The error associated with three-dimensional e¤ects in the wind tunnel outweighed the di¤erences between the CFD results making it impossible to discern between the performances of the turbulence models tested. While the SST model is perceived to be the most suitable turbulence model for ‡ows with mild separation, little can be said here about its suitability for highly separated ‡ows.

It is highly likely that the sail section data presented by Milgram (1971, 1978) is a¤ected by similar three-dimensional e¤ects. Milgram notes that wall e¤ects are neglected and that it was impossible to estimate the in‡uence that non-uniform ‡ow separation would have on the results. Milgram's model had

an aspect ratio of just 2.2 and there were 1.6*mm* gaps at the tips. The models tested by Wilkinson (1984, 1989, 1990) had an aspect ratio of 3.0 and hense, for the high camber sections (up to 20% camber) at least, some degree of three-dimensionality must have exisited in the wake. However Wilkinson's data was in the form of pressure coe¢cient measurements and boundary layer pro…les at the midspan of the model and it is possible that three-dimesional e¤ects are isolated near the walls and the ‡ow at midspan was nominally two-dimensional. Wilkinson con…rmed this by comparing pressure distributions three di¤erent spanwise locations. Unfortunately the data recorded by Wilkinson does not include velocity and turbulence measurements within the leading and trailing edge separation regions. Without such data it is di¢cult to compare turbulence models and to understand the physical and mathematical reasons for their relative performance. Also the models tested by Wilkinson were derived from upwind sail designs and have less camber than downwind sails, consequently the data compiled by Wilkinson is not ideal for the validation of turbulence models for downwind sail design.

Clearly the wind tunnel tests presented in this chapter are insu¢cient for validation of CFD results and it was evident at the completion of the project that further wind tunnel tests were required. From the results of this preliminary study it was concluded that signi…cant changes to the setup and measurement techniques would be necessary for subsequent wind tunnel tests; they are:

1. High aspect ratio sections are required in order to minimise three-dimensional e¤ects. CFD simulations can be used to determine suitable aspect ratios.

2. A larger wind tunnel was required in order to obtain higher aspect ratios whilst maintaining practical chord lengths for resolution of measurement techniques and to maintain a convenient Reynolds number.

3. Measurements need to be conducted at midspan in order to remove errors associated with three-dimensional e¤ects at the model/wall junction, i.e., no span-averaged measurements of lift, drag etc.

4. Velocity and turbulent stress measurements are required in order to provide a more detailed understanding of sail ‡ows. In particular the physics of the leading and trailing edge separation regions as well as the boundary layer leading up to the trailing edge separation point need to be understood better.

These conclusions were used to form the strategy for the wind tunnel tests carried out at NASA Ames in conjunction with Stanford Yacht Research and the Center for Turbulence Reseach at Stanford University. The results of these tests are presented in the next chapter.

Bibliography

[1] M. J. Crompton, *The Thin Aerofoil Leading Edge Bubble*, Ph.D. thesis, University of Bristol, 2001.

[2] F. R. Menter, "Two-equation turbulence models for aerodynamic ‡ows," *Journal of Fluid Dynamics - Transactions of the ASME*, vol. 118, pp. 514–519, 1996.